ation of a class of infectivity-enhanced adenoviral vectors in ovarian cancer gene therapy, Gene Ther. 11 (2004) 874–878.

[30] Y. Okada, N. Okada, S. Nakagawa, H. Mizuguchi, K. Takahashi, N. Mizuno, T. Fujita, A. Yamamoto, T. Hayakawa, T. Mayumi, Tumor necrosis factor α-gene therapy for an established murine melanoma using RGD (Arg-Gly-Asp) fiber-mutant adenovirus vectors, Jpn. J. Cancer Res. 93 (2002) 436–444.

[31] J.Q. Gao, S. Inoue, Y. Tsukada, K. Katayama, Y. Eto, S. Kurachi, H. Mizuguchi, T. Hayakawa, Y. Tsutsumi, T. Mayumi, S. Nakagawa, High gene expression of mutant adenovirus vector both in vitro and in vivo with the insertion of integrin-targeting peptide into the fiber, Pharmazie 59 (2004) 571–572.

[32] J.P. Leonard, M.L. Sherman, G.L. Fisher, L.J. Buchanan, G. Larsen, M.B. Atkins, J.A. Sosman, J.P. Dutcher, N.J. Vogelzang, J.L. Ryan, Effects of single-dose interleukin-12 exposure on interleukin-12-associated toxicity and interferon-gamma production, Blood 90 (1997) 2541–2548.

[33] S. Sacco, H. Heremans, B. Hchtenacher, W.A. Buurman, Z. Amraoui, M. Goldman, P. Ghezzi, Protective effect of a single interleukin-12 (IL-12) predose against the toxicity of subsequent chronic IL-12 in mice: Role of cytokines and glucocorticoids, Blood 90 (1997) 4473–4479.

[34] C. Lechanteur, M. Moutschen, F. Princen, M. Lopez, E. Franzen, J. Gielen, V. Bours, M.P. Merville, Antitumoral vaccination with granulocyte-macrophage colony-stimulating factor or interleukin-12-expressing DHD/K12 colon adenocarcinoma cells, Cancer Gene Ther. 7 (2000) 676–682.

[35] L. Zitvogel, B. Couderc, J.I. Mayordomo, P.D. Robbins, M.T. Lotze, W.J. Storkus, IL-12-engineered dendritic cells serve as effective tumor vaccine adjuvants in vivo, Ann. N.Y. Acad. Sci. 795 (1996) 284–293.

[36] G. Mazzolini, C. Qian, X. Xie, Y. Sun, J.J. Lasarte, M. Drozdzik, J. Prieto, Regression of colon cancer and induction of antitumor immunity by intratumoral injection of adenovirus expressing interleukin-12, Cancer Gene Ther. 6 (1999) 514–522.

[37] M. Caruso, K. Pham Nguyen, Y.L. Kwong, B. Xu, K.I. Kosai, M. Finegold, S.L. Woo, S.H. Chen, Adenovirus-mediated interleukin-12 gene therapy for metastasis colon carcinoma, Proc. Natl. Acad. Sci. USA 93 (1996) 11302–11306.

[38] E.T. Akporiaye, E. Hersh, Clinical aspects of intratumoral gene therapy, Curr. Opin. Mol. Ther. 1 (1999) 443–453.

[39] H. Fujiwara, N. Yamauchi, Y. Sato, K. Sasaki, M. Takahashi, T. Okamoto, T. Sato, S. Iyama, Y. Koshita, M. Hirayama, H. Yamagishi, Y. Niitsu, Synergistic suppressive effect of double transfection of tumor necrosis factor-α and interleukin 12 genes on tumorigenicity of Meth-A cells, Jpn. J. Cancer Res. 91 (2000) 1296–1302.

[40] Y. Okada, N. Okada, H. Mizuguchi, K. Takahashi, T. Hayakawa, T. Mayumi, N. Mizuno, Optimization of antitumor efficacy and safety of in vivo cytokine gene therapy using RGD fiber-mutant adenovirus vector for preexisting murine melanoma, Biochim. Biophys. Acta 1670 (2004) 172–180.

[41] G. Mazzolini, J. Prieto, I. Melero, Gene therapy of cancer with interleukin 12, Curr. Pharm. Des. 9 (2003) 1981–1991.

THE JOURNAL OF GENE MEDICINE
J Gene Med 2005; 7: 604–612.
Published online 15 November 2004 in Wiley InterScience (www.interscience.wiley.com). **DOI:** 10.1002/jgm.699

RESEARCH ARTICLE

PEGylated adenovirus vectors containing RGD peptides on the tip of PEG show high transduction efficiency and antibody evasion ability

Yusuke Eto[1†]
Jian-Qing Gao[1,2†]
Fumiko Sekiguchi[1]
Shinnosuke Kurachi[1]
Kazufumi Katayama[1]
Mitsuko Maeda[4]
Koichi Kawasaki[4]
Hiroyuki Mizuguchi[3]
Takao Hayakawa[3]
Yasuo Tsutsumi[3]
Tadanori Mayumi[4]
Shinsaku Nakagawa[1]*

[1]*Graduate School of Pharmaceutical Sciences, Osaka University, Japan*

[2]*College of Pharmaceutical Sciences, Zhejiang University, P.R. China*

[3]*National Institute of Health Sciences, Japan*

[4]*School of Pharmaceutical Sciences, Kobe Gakuin University, Japan*

*Correspondence to:
Shinsaku Nakagawa, Department of Biopharmaceutics, Graduate School of Pharmaceutical Sciences, Osaka University, Yamadaoka 1-6, Suita City, Osaka 565-0871, Japan.
E-mail:
nakagawa@phs.osaka-u.ac.jp

†These authors contributed equally to this work.

Received: 14 June 2004
Revised: 2 September 2004
Accepted: 2 September 2004

Abstract

Background PEGylation of adenovirus vectors (Ads) is an attractive strategy in gene therapy. Although many types of PEGylated Ad (PEG-Ads), which exhibit antibody evasion activity and long plasma half-life, have been developed, their entry into cells has been prevented by steric hindrance by polyethylene glycol (PEG) chains. Likewise, sufficient gene expression for medical treatment could not be achieved.

Methods A set of PEG-Ads, which have different PEG modification rates, was constructed, and gene expression was evaluated using A549 cells. A novel PEGylated Ad (RGD-PEG-Ad), which contained RGD (Arg-Gly-Asp) peptides on the tip of PEG, was developed. We evaluated gene expression both in Coxsackie-adenovirus receptor (CAR)-positive as well as -negative cells, and *in vivo* gene expression was also determined. Furthermore, the antibody evasion ability and the specificity of infection exhibited by this RGD-PEG-Ad were also evaluated.

Results Whereas PEG-Ads decreased gene expression in CAR-positive cells, RGD-PEG-Ad enhanced gene expression notably, to a level about 200-fold higher than that of PEG-Ads. Moreover, gene expression of RGD-PEG-Ad was almost equal to that of Ad-RGD, which contains an RGD-motif in the fiber and exhibits among the highest gene expression of CAR-positive and -negative cells. Furthermore, although Ad-RGD gene expression decreased remarkably in the presence of anti-Ad antiserum, RGD-PEG-Ad maintained its activity against antibodies. *In vivo* experiments also demonstrated that the modification of Ads with RGD-PEG induced efficient gene expression.

Conclusions In the present study, we demonstrated that a new strategy, which combined integrin-targeting the RGD peptide on the tip of PEG and modified the Ad using this material, could enhance gene expression in both CAR-positive and -negative cells. At the same time, this novel PEGylated Ad maintained strong protective activity against antibodies. This strategy could also be easily modified for developing other vectors using other targeting molecules. Copyright © 2004 John Wiley & Sons, Ltd.

Keywords adenovirus; antibody; polyethylene glycol; RGD peptide; gene expression

Introduction

Gene therapy for cancer or other incurable diseases has attracted considerable attention. The major obstacle to widespread utilization of gene therapy

involves the transgenic vector. Adenovirus vectors (Ads) exhibit high transduction efficiency and gene expression, and can efficiently transfer genes into both dividing and non-dividing cells. Therefore, they are widely used as vectors for gene therapy [1–4]. On the other hand, many people carry neutralizing antibodies to Ads, and the administration of a large amount of Ads may cause side effects. Therefore, clinical application of Ads is difficult [5,6], and many studies have been conducted in an attempt to overcome the limitations of Ads [7–9].

PEGylation, the covalent attachment of activated monomethoxy polyethylene glycol to free lysine groups on the surface of an Ad, is a promising strategy for overcoming these limitations. PEGylation of therapeutic proteins such as cytokines has been reported previously [10,11], and several groups have reported that PEGylated adenovirus exhibits several advantageous attributes [12–14]. Without the need for modifying Ad capsid protein by genetic recombination, a PEGylated Ad (PEG-Ad) can transduce its therapeutic gene into cells even in the presence of Ad-neutralizing antibodies [15,16], and extend residence time in the blood [17]. Furthermore, targeting of PEG-Ads has also been attempted. Lanciotti *et al.* reported targeting Ads using heterofunctional PEG, tresyl-PEG-maleimide [18]. Conjugation of optimized fibroblast growth factor 2 (FGF2), which possesses monoreactive cysteine, to the maleimide group on PEG-Ad was mediated by a reactive sulfhydryl group on the surface of the protein. Ogawara *et al.* reported enhanced transgene delivery to activated vascular endothelial cells using a PEG-Ad combined with an antibody on the tip of PEG [19]. These reports suggest that the use of a functional molecule on the tip of PEG can efficiently change the tropism of Ads or PEG-Ads.

In the present study, we attempted to overcome the previously observed reduction in gene expression caused by the inhibition of endocytosis through the Coxsackie-adenovirus receptor (CAR). This inhibition is due to steric hindrance by the PEG chains and has prevented the widespread therapeutic use of PEG-Ads. Therefore, we developed a new versatile Ad that maintained the positive attributes of PEGylation but also exhibited high transduction efficiency both in CAR-positive and -negative cells.

Infection by Ads occurs in two distinct steps. In the first step, the fiber protein of the Ad binds to its CAR [20–22], and the transduction efficiency of this step is influenced by the amount of CAR present. Following this, internalization via receptor-mediated endocytosis is promoted when the RGD motif of the penton bases combines with $\alpha v\beta 3$ and $\alpha v\beta 5$ integrins [23,24], which are present on many types of cells. We focused on the second step of Ad infection and constructed PEG with RGD peptides on the tip. The PEGylated Ad (RGD-PEG-Ad), which contained RGD peptide on the tip of PEG, was expected to show high transduction efficiency for both CAR-positive and -negative cells because of the interaction between RGD and integrin. Likewise, RGD-PEG-Ad possesses the ability to avoid neutralizing antibodies, a major advantage of PEGylation [15,16]. Incidentally, an Ad that contains an RGD peptide in the HI loop of the fiber (Ad-RGD) has already been developed, and this vector exhibits the highest transduction efficiency via integrin [25,26].

In the present study, we constructed several PEG-Ads at various PEG modification rates, and measured their gene expression. Following this, we used Lipofectamine to determine whether PEG-Ads possessed high gene expression ability. This verified that, upon entering a cell, PEG-Ad expressed the gene originating from the Ad itself. In the next step, we constructed RGD-PEG-Ad and measured its gene expression in CAR-positive and -negative cells with or without Ad antiserum.

Materials and methods

Cell lines

A549 (human lung carcinoma) cells were cultured in Dulbecco's modified Eagle's medium supplemented with 10% fetal calf serum (FCS). B16BL6 (mouse melanoma) cells were cultured in minimum essential medium supplemented with 7.5% FCS.

Development of adenovirus vectors

In this study, all experiments used E1-deleted Ad type 5, which expressed firefly luciferase under the control of cytomegalovirus (CMV) promoters. Both conventional and RGD fiber mutant Ads were amplified in 293 cells using a modification of established methods, purified from cell lysates by banding twice through CsCl gradients, dialyzed and stored at −80 °C. The Ads used in this study were constructed by an improved *in vitro* ligation method as described previously [27]. Determination of virus particle titer was accomplished spectrophotometrically by the methods of Maizel *et al.* [28].

Preparation of RGD-PEG

The synthetic scheme for RGD-PEG is shown in Figure 3. *N*-(9-Fluorenylmethoxycarbonyl)-*O*-(succimidyl)-ω-amino-α-carboxy-PEG (Fmoc-PEG-NHS, MW 3400) was purchased from Shearwater Corporation (USA). β-Ala (βA) was used as a spacer between PEG and the RGD peptide. (Ac-YGGRGDTPβA)$_2$K-PEG-βAC-amide (RGD-PEG, MW 5500) was synthesized manually on a Rink amide resin [29] using a 9-fluorenylmethoxycarbonyl (Fmoc)-based solid-phase strategy. We employed 2(1*H*-benzotriazol-1-yl)-1,1,3,3-tetramethyluronium hexafluorophosphate and 1-hydroxybenzotriazole as coupling reagents, trityl (Trt) protection as the sulfhydryl group source, *tert*-butyl as the hydroxyl group source and 2,2,5,7,8-pentamethylchroman-6-sulfonyl (Pmc) protection as the guanidinyl group source. To liberate the synthetic RGD-PEG from the resin, cleavage was achieved by using

a mixture of trifluoroacetic acid/triisopropylsilane/H_2O (95 : 2.5 : 2.5) [30] for 2 h at room temperature, followed by high-performance liquid chromatography (HPLC) purification on a C18 column. After addition of the peptide to *N*-(6-maleimidecaproyloxy)succinimide) (EMCS) in phosphate-buffered saline (PBS), pH 6.4, the solution was changed to pH 7.4 PBS and kept frozen at −80 °C.

Covalent attachment of PEG to Ads

Activated methoxypolyethylene glycol-succinimidyl propionate (mPEG-SPA, MW 5000; Shearwater Corporation, USA) and RGD-PEG were used in this study. Ads were reacted with 25–6400-fold molar excess of mPEG-SPA to viral lysine residue at 37 °C for 45 min with gentle stirring. Ads were also reacted with 250-fold molar excess of RGD-PEG under the same conditions. CsCl gradient ultracentrifugation was used for PEGylated adenovirus purification, and we assessed whether unmodified Ads were mixed with the PEGylated Ad. Modification ratio of PEGylated-Ads was determined by sodium dodecyl sulfate/polyacrylamide gel electrophoresis (SDS-PAGE) analysis using NIH image software. SDS-PAGE was carried out, referring to the previous report by O'Riordan *et al.* [15], in a 4–20% polyacrylamide gel (PAG Mini 4/20; Daiichi Pure Chemicals, Japan). Viral protein (hexon) was stained by Coomassie brilliant blue. The PEGylated hexon band was separated from the unmodified hexon band. The ratios of each band were measured using NIH Image software, and the PEG modification ratio was calculated as described below, the band of PEGylated hexon/the band of PEGylated and unmodified hexon ×100 [16]. After dilution in PBS, the particle sizes of Ads and RGD-PEG-Ad were measured using a Zetasizer 3000HS (Malvern Inc. UK).

Transduction efficiency of PEGylated Ads into A549 cells

A549 cells (2×10^4 cells/well) were seeded onto a 48-well plate. On the following day, the cells were transduced with 300, 1000, 3000, or 10 000 particles/cell of unmodified Ads and PEG-Ads that possessed various PEG modifications in a final volume of 500 µl in cell medium. After 24 h cultivation, luciferase activity was measured using the luciferase assay system (Promega, USA) and Microlumat Plus LB 96 (Perkin Elmer, USA) after cells had been lysed with the luciferase cell culture lysis reagent (Promega, USA). Luciferase activity was calculated as relative light units (RLU)/well. In the presence of 20 µg/ml Lipofectamine 2000 (Invitrogen, USA), A549 cells were transduced with 1000 particles/cell of unmodified Ads, 43%, 72%, and 89% modified PEG-Ads, heatinactivated Ads, or heat-inactivated PEG-Ads, respectively. After 4 h, the virus solution was replaced with fresh medium, and the cells were incubated for 24 h. Subsequently, luciferase expression was measured using the method described above.

Transduction efficiency of RGD-PEG-Ad into A549 and B16BL6 cells

A549 and B16BL6 cells (2×10^4 cells/well) were seeded onto a 48-well plate. On the following day, the cells were transduced with 300, 1000, 3000, and 10 000 particles/cell of unmodified Ads, PEG-Ads, RGD-PEG-Ad or Ad-RGD, respectively, in a final volume of 500 µl in cell medium. After 24 h cultivation, luciferase activity was measured using the method described above.

Competition experiments using RGD peptide

B16BL6 cells (2×10^4 cells/well) were seeded onto a 48-well plate. On the following day, cells were incubated with RGD peptide (GRGDTP, SIGMA) at a final concentration of 200 µg/ml for 10 min at room temperature, and then 3000 particles/cell of unmodified Ads, RGD-PEG-Ad or Ad-RGD were added to a final volume of 300 µl in cell medium. After 24 h cultivation, luciferase activity was measured using the method described above.

Preparation of Ad antiserum

Ad antiserum was obtained from ICR mice using methods previously reported by us and others [16,31]. In brief, a dose of 10^{10} particles of unmodified Ad containing Freund's complete adjuvant in 100 µl of PBS was administered hypodermically to a female ICR mouse (6 weeks old). Two to four weeks later, an additional dose of 10^{10} viral particles in Freund's incomplete adjuvant was hypodermically administered. Mouse serum was collected after 1 week, and stored at −20 °C.

Antibody evasion by RGD-PEG-Ad in B16BL6 cells

B16BL6 cells (2×10^4 cells/well) were seeded onto a 48-well plate. On the following day, the cells were transduced with 1000 particles/cell of RGD-PEG-Ad or Ad-RGD in a final volume of 500 µl in cell medium in the presence or absence of 100 µl/well Ad antiserum (42, 125 ng protein/well). After 24 h cultivation, luciferase activity was measured using the method described above.

Ad-mediated gene transduction *in vivo*

Unmodified Ad, Ad-RGD, and RGD-PEG-Ad (1.5×10^{10} particles/100 µl) were intravenously injected into BALB/c mice (female, 6 weeks old; obtained from Nippon SLC, Kyoto, Japan). Forty-eight hours later, organs were isolated and homogenized as previously described [32]. Luciferase activity was measured using the method described above.

Statistical analysis

Student's t-test was used for statistical comparison when applicable. Differences were considered statistically significant at $P \leq 0.05$.

Results

Transduction efficiency of Ads declines in response to PEGylation

We confirmed the feasibility of constructing PEG-Ads that exhibit various PEG modification rates, which are regulated by the amount of PEG made available for the reaction (data not shown). In the present study, Ads were reacted with 25-, 100-, 400-, 1600- and 6400-fold molar excesses of PEG relative to viral lysine residue. The results showed that the transduction efficiency of PEG-Ads fell remarkably as the PEG modification rate increased (Figure 1). Luciferase expression of the 34% modified PEG-Ad was approximately 200-fold lower than that of unmodified Ads, and gene expression of the 89% modified PEG-Ad fell by 100 000 or more and was not dose-dependent.

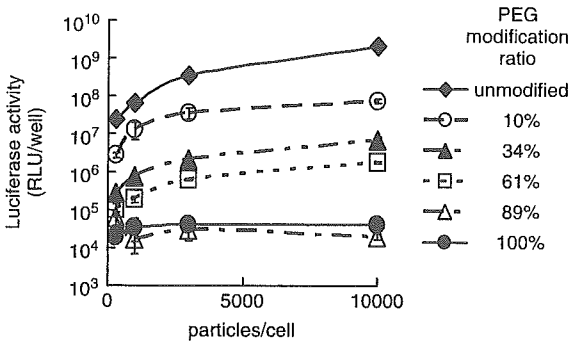

Figure 1. Transduction efficiency of PEGylated adenovirus vectors into A549 cells. A549 cells (2×10^4 cells) were transduced with 300, 1000, 3000 or 10 000 particles/cell of unmodified Ad or PEG-Ad encoding the luciferase gene at the indicated modification ratios. Luciferase expression was measured after 24 h. Each point represents the mean ± S.D. (n = 3)

PEG-Ads show high gene expression upon cell entry

We introduced PEG-Ads into cells using Lipofectamine and measured their gene expression in order to verify that the decrease of gene expression of PEG-Ads was derived from binding inhibition due to steric hindrance by PEG chains. The results shown in Figure 2 demonstrated that, in the absence of Lipofectamine, the transduction efficiency of PEG-Ads significantly decreased as PEG modification rate increased. However, in the presence of Lipofectamine, PEG-Ad gene expression at 43% modification was enhanced significantly to nearly that of unmodified Ads. Even at high modification rates (89%), the PEG-Ad gene expression in the presence of Lipofectamine was more than 130-fold higher than that in the absence of Lipofectamine. The gene expression of the heat-inactivated unmodified Ads and the heat-inactivated PEG-Ads were very low even with Lipofectamine. The results

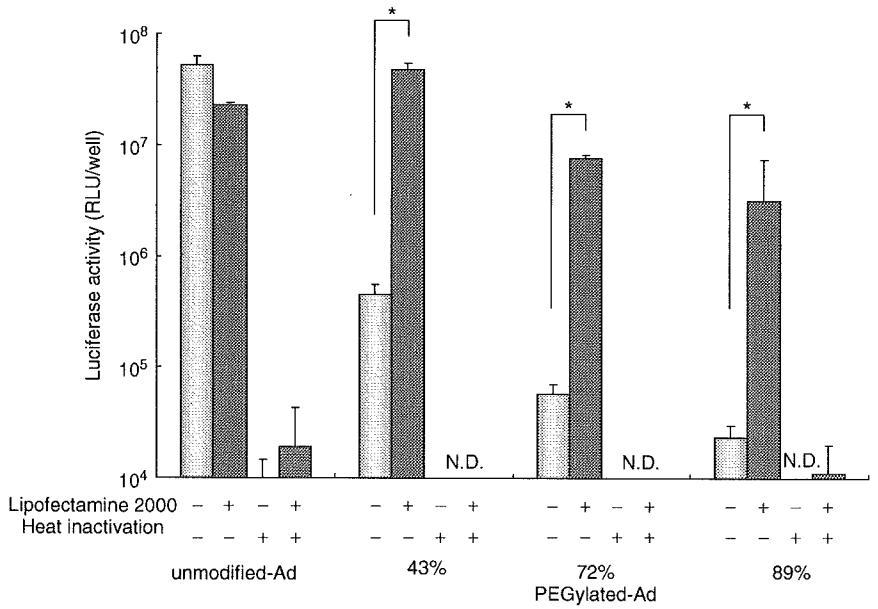

Figure 2. Transduction efficiency of PEGylated adenovirus vectors into A549 cells in the presence or absence of Lipofectamine 2000. A549 cells (2×10^4 cells) were transduced with 1000 particles/cell of unmodified Ad or PEG-Ad in the presence or absence of 20 μg/ml of Lipofectamine 2000. After 4 h, the virus solution was replaced with fresh medium, and the cells were incubated for 24 h. Luciferase expression was measured. Each point represents the mean ± S.D. (n = 3). *$P < 0.05$ (Student's t-test)

shown here indicate that high transduction efficiency, which is characteristic of Ads, decreased due to the steric hindrance of CAR by PEG chains.

Construction of PEGylated Ads with RGD peptides

In selecting the adhesion molecule, we focused on the RGD motif, the second mediator of Ad internalization. We constructed RGD-PEG-Ad using RGD-PEG-NHS (Figure 3), which contains two RGD motifs (YGGRGDTP) on the tip of PEG, and we investigated the characteristics of RGD-PEG-Ad (Table 1). RGD-PEG-Ad was 12.5 nm bigger in diameter than unmodified Ads, and the PEG modification rate (36%) was confirmed by SDS-PAGE and NIH Image software.

Enhanced transduction efficiency of RGD-PEG-Ad in comparison to that induced by PEG-Ads

We compared the transduction efficiency of unmodified Ads, PEG-Ads, Ad-RGD, and RGD-PEG-Ad in both A549 (CAR-positive) and B16BL6 (CAR-negative) cells. In A549 cells, RGD-PEG-Ad showed 100-fold higher gene expression than PEG-Ad, which exhibits the same level of modification. This gene expression level was similar to that of unmodified Ads and Ad-RGD (Figure 4A). In B16BL6 cells, RGD-PEG-Ad exhibited 60-fold and 200-fold higher gene expression rates than unmodified Ad and PEG-Ad, respectively, but the expression rate was similar to that of Ad-RGD (Figure 4B).

Table 1. Modification ratio and vectors size of RGD-PEG-Ad

Ratio (Ad/RGD-PEG)*	PEG modification ratio (%)	Vector size (nm)
1:0 (unmodified)	0	122.1 ± 4.5
1:250	36	134.6 ± 2.7

*Amount of PEG to lysine residue of adenovirus vector capsid protein (mol/mol)

RGD-PEG-Ad specifically infect cells through integrin

The specificity of RGD-PEG-Ad binding via integrin was evaluated by competition assay using the RGD peptide, GRGDTP, which has been widely used as a competitive peptide for integrin [33,34]. In the presence of GRGDTP, RGD-PEG-Ad and Ad-RGD gene expression was remarkably decreased compared to that in the absence of RGD peptide (Figure 5). In contrast, unmodified Ad did not decrease notably, suggesting the introduction of RGD-PEG-Ad was integrin-dependent.

RGD-PEG-Ad maintains its high gene expression in the presence of Ad antiserum

We evaluated transduction efficiency of Ad-RGD and RGD-PEG-Ad in the presence or absence of Ad antiserum using B16BL6 cells. In the presence of Ad antiserum, Ad-RGD gene expression was reduced remarkably. However, RGD-PEG-Ad maintained its high transduction efficiency (Figure 6). In the presence of 125 ng anti-Ad antibody,

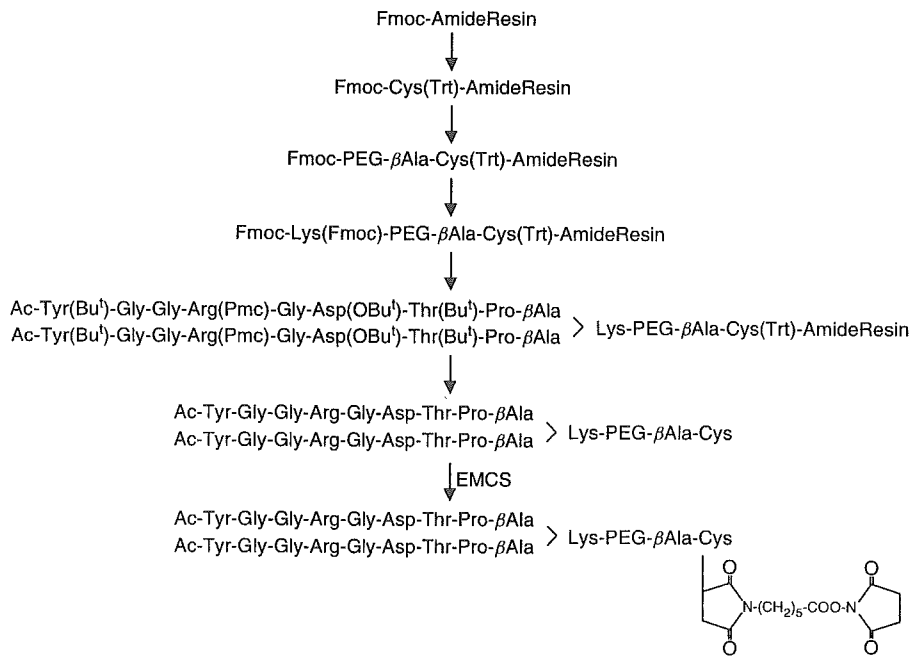

Figure 3. Structural scheme for RGD-PEG

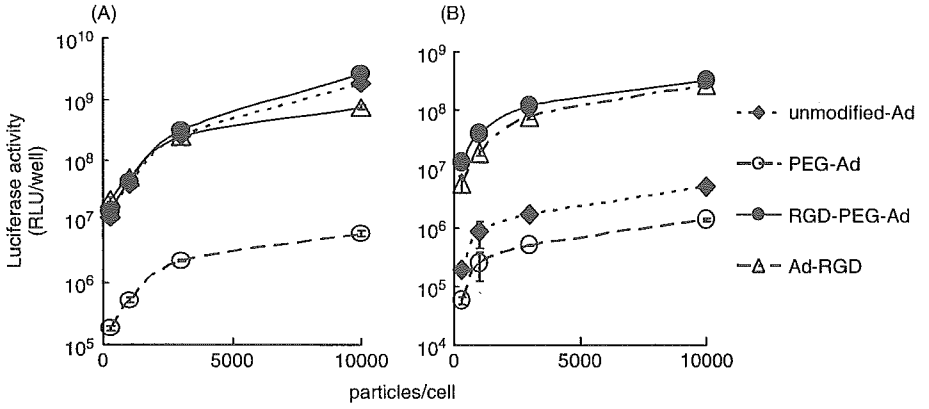

Figure 4. Transduction efficiency of RGD-PEGylated adenovirus vectors into A549 cells and B16BL6 cells. (A) A549 (2×10^4) cells and (B) B16BL6 cells (2×10^4) were transduced with 300, 1000, 3000 or 10 000 particles/cell of unmodified Ad, PEG-Ad, RGD-PEG-Ad or Ad-RGD, respectively. Luciferase expression was measured after 24 h. Each point represents the mean ± S.D. (n = 3)

RGD-PEG-Ad retained more than one-tenth of its activity, whereas Ad-RGD lost more than 99% of its activity in the absence of antibody.

RGD-PEG-Ad possessed high gene expression *in vivo*

Unmodified Ad, Ad-RGD, and RGD-PEG-Ad mediated luciferase activity predominantly in the liver after intravenous administration. No significant difference in liver transduction was found between unmodified Ad and RGD-PEG-Ad (Figure 7). Biodistribution of Ad-RGD and RGD-PEG-Ad was similar in lung, spleen, kidney, heart and brain (data not shown).

Discussion

Ads are widely used as vectors for gene therapy experiments. To date, several methods including gutless Ads, which address the decrease in antigenicity [35–37], and fiber mutant Ads [25,38,39], have been developed. In the present study, we initially focused on the modification of Ads by PEG because of its relative ease of development and many other merits such as evasion of neutralizing antibodies. However, as is well known, the conjugation of an Ad with high molecular weight material hinders its interaction with its receptor and subsequently influences the introduction of the virus. Therefore, our aim was to develop novel vectors that exhibit high gene expression while at the same time maintaining the other merits of PEGylated-Ads.

PEGylation of proteins and liposomes has already been widely employed and increased blood stability and mitigation of side effects have been reported [10,11]. PEGylation of the surface of Ads has several advantages. We and other groups have previously demonstrated that modification of an Ad with PEG protects it from neutralizing antibodies [15,16,31]. Likewise, PEGylation has been reported to extend the half-life of Ads in blood

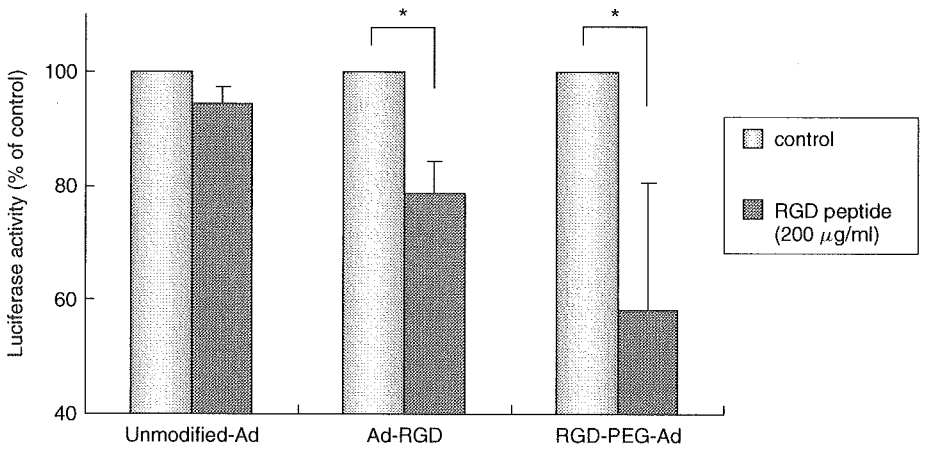

Figure 5. Transduction efficiency of RGD-PEGylated adenovirus vectors in the presence or absence of RGD peptide. B16BL6 cells (2×10^4) were transduced with 3000 particles/cell of unmodified Ad, Ad-RGD or RGD-PEG-Ad in the presence or absence of RGD peptide (200 μg/ml). Luciferase expression was measured after 24 h. Each point represents the mean ± S.D. (n = 3). *$P < 0.05$ (Student's t-test)

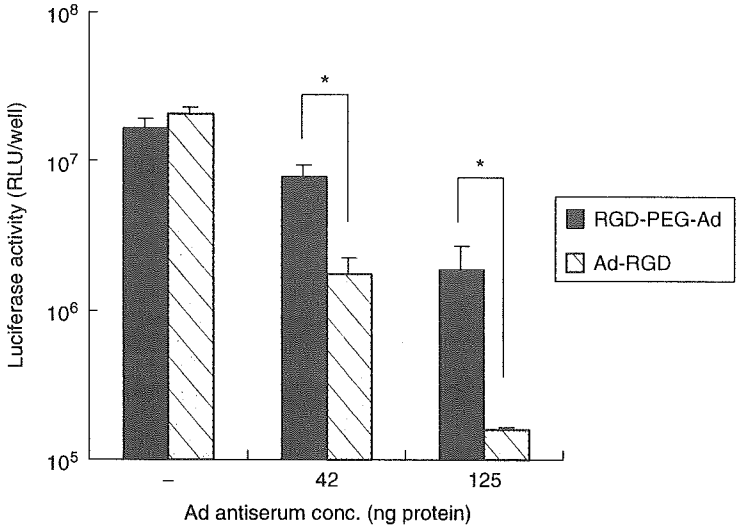

Figure 6. Transduction efficiency of RGD-PEGylated adenovirus vectors in the presence of adenovirus vector antiserum. B16BL6 cells (2×10^4) were transduced with 1000 particles/cell of RGD-PEG-Ad or Ad-RGD in the presence or absence of Ad antiserum. Luciferase expression was measured after 24 h. Each point represents the mean ± S.D. (n = 3). *$P < 0.05$ (Student's t-test)

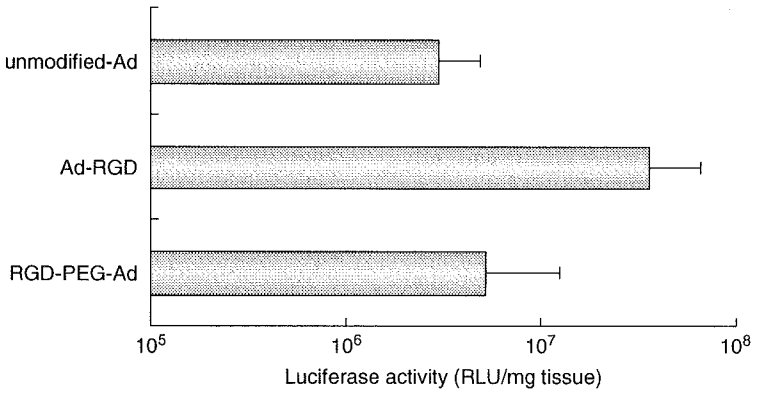

Figure 7. The gene expression in liver induced by RGD-PEG-Ad. 1.5×10^{10} particles of unmodified Ad, Ad-RGD, or RGD-PEG-Ad were injected intravenously. After 2 days, the liver was harvested and homogenized. Luciferase activity was then measured using the kit according to the manufacturer's instructions. Each point represents the mean ± S.D. (n = 4)

[17]. Steric hindrance by PEG chains and masking of the Ad surface electric charge were expected to reduce uptake by Kuppfer cells. In the present study, we established a method that can control the rate of Ad modification, and the results confirmed that PEGylation notably reduced gene expression efficiency in A549 cells. The data also suggest that increased modification with PEG induced lower gene expression (Figure 1).

In a clinical setting, the most serious problem associated with PEG-Ads is the decrease in transduction. We determined that this decrease results from the inhibition of Ad and CAR interaction due to steric hindrance by PEG chains (Figure 2). This suggests that high gene expression can be achieved if PEGylated-Ads can be transduced into cells. Therefore, in the present study, we focused on the RGD motif, which mediates the entrance of Ads into cells following the interaction with integrin [23,24]. We initially constructed RGD-PEG, which contains the RGD peptide at the tip of PEG, and reacted it with Ad to form RGD-PEG-Ad. The data in Table 1 demonstrate that the vector size of RGD-PEG-Ad was 12 nm bigger than that of unmodified Ad, and the same tendency was observed in the case of PEG-Ads. The size of Ads increased to about 10–15 nm at a PEG modification rate of 30–40% (data not shown). We thereby succeeded in developing a novel PEG-Ad, the efficacy of which was not influenced by the combination with PEG.

RGD-PEG-Ad gene expression in A549 cells was significantly higher than that of PEG-Ad, and was equivalent to conventional Ad and Ad-RGD (Figure 4). In CAR-negative B16BL6 cells, RGD-PEG-Ad also showed enhanced gene expression, which was much higher than that of PEG-Ads or conventional Ads. Because CAR is expressed at low levels in certain cells, such as hematopoietic stem cells, peripheral blood cells, differentiated airway epithelium, muscle cells, most mouse-derived cells, and many tumor cells, this novel PEGylated Ad is attractive for gene therapy. In addition,

our RGD-PEG-Ad was very stable under −80 °C storage conditions, despite several cycles of freezing and thawing (data not shown).

We also checked the specificity of RGD-PEG-Ad infection; we measured the gene expression of unmodified Ad, Ad-RGD, and RGD-PEG-Ad in the presence or absence of competitive RGD peptide (Figure 5). Koizumi *et al.* [25] have already reported the specificity of infection of Ad-RGD through integrin. In the present study, RGD-PEG-Ad gene expression was significantly inhibited by RGD peptide, GRGDTP, and, because RGD-PEG-Ad gene expression in CAR-negative, integrin-positive cells was notably enhanced compared to that of PEG-Ad, we suggest that the transduction of RGD-PEG-Ad was integrin-dependent.

Moreover, we determined whether RGD-PEG-Ad improved resistance to neutralizing antibodies (Figure 6). The expression of Ad-RGD genes fell remarkably in the presence of Ad antiserum. However, we demonstrated that RGD-PEG-Ad gene expression was far higher than that of Ad-RGD in the presence of the antiserum. This ability to evade antibodies is essential for clinical applications because nearly 80% of human patients possess anti-Ad antibodies, and re-administration is indispensable in some cases. Therefore, RGD-PEG-Ad minimizes the amount of medication required and reduces side effects.

The method described here is also applicable to other virus vectors and other target molecules. We are currently screening the use of peptides or antibodies as antigens or tissue-specific targeting molecules using the phage display system. These approaches will promote the development of a virus vector that exhibits enhanced safety and applicability.

Acknowledgements

This study was supported in part by the Research on Health Sciences focusing on Drug Innovation from The Japan Health Sciences Foundation; by Grants-in-Aid for Exploratory Research from the Ministry of Education, Culture, Sports, Science and Technology of Japan; and by grants from the Ministry of Health and Welfare in Japan.

References

1. Gao JQ, Tsuda Y, Katayama K, *et al.* Antitumor effect by interleukin-11 receptor alpha-locus chemokine/CCL27, introduced into tumor cells through a recombinant adenovirus vector. *Cancer Res* 2003; **63**: 4420–4425.
2. Crystal RG. Transfer of genes to humans: early lessons and obstacles to success. *Science* 1995; **270**: 404–410.
3. Wilson JM. Adenoviruses as gene-delivery vehicles. *N Engl J Med* 1996; **334**: 1185–1187.
4. Smith TA, Mehaffey MG, Kayda DB, *et al.* Adenovirus mediated expression of therapeutic plasma levels of human factor IX in mice. *Nat Genet* 1993; **5**: 397–402.
5. Wohlfart C. Neutralization of adenoviruses: kinetics, stoichiometry, and mechanisms. *J Virol* 1988; **62**: 2321–2328.
6. Mastrangeli A, Harvey BG, Yao J, *et al.* "Sero-switch" adenovirus-mediated in vivo gene transfer: circumvention of anti-adenovirus humoral immune defenses against repeat adenovirus vector administration by changing the adenovirus serotype. *Hum Gene Ther* 1996; **7**: 79–87.
7. Mizuguchi H, Koizumi N, Hosono T, *et al.* A simplified system for constructing recombinant adenoviral vectors containing heterologous peptides in the HI loop of their fiber knob. *Gene Ther* 2001; **8**: 730–735.
8. Yei S, Mittereder N, Tang K, *et al.* Adenovirus-mediated gene transfer for cystic fibrosis: quantitative evaluation of repeated in vivo vector administration to the lung. *Gene Ther* 1994; **1**: 192–200.
9. Croyle MA, Yu QC, Wilson JM. Development of a rapid method for the PEGylation of adenoviruses with enhanced transduction and improved stability under harsh storage conditions. *Hum Gene Ther* 2000; **11**: 1713–1722.
10. Tsutsumi Y, Tsunoda S, Kamada H, *et al.* Molecular design of hybrid tumour necrosis factor-alpha. II. The molecular size of polyethylene glycol-modified tumour necrosis factor-alpha affects its anti-tumour potency. *Br J Cancer* 1996; **74**: 1090–1095.
11. Yoshioka Y, Tsutsumi Y, Ikemizu S, *et al.* Optimal site-specific PEGylation of mutant TNF-alpha improves its antitumor potency. *Biochem Biophys Res Commun* 2004; **315**: 808–814.
12. Romanczuk H, Galer CE, Zabner J, *et al.* Modification of an adenoviral vector with biologically selected peptides: a novel strategy for gene delivery to cells of choice. *Hum Gene Ther.* 1999; **1**: 2615–2626.
13. Croyle MA, Chirmule N, Zhang Y, *et al.* "Stealth" adenoviruses blunt cell-mediated and humoral immune responses against the virus and allow for significant gene expression upon readministration in the lung. *J Virol* 2001; **75**: 4792–4801.
14. Croyle MA, Chirmule N, Zhang Y, *et al.* PEGylation of E1-deleted adenovirus vectors allows significant gene expression on readministration to liver. *Hum Gene Ther* 2002; **10**: 1887–1900.
15. O'Riordan CR, Lachapelle A, Delgado C, *et al.* PEGylation of adenovirus with retention of infectivity and protection from neutralizing antibody in vitro and in vivo. *Hum Gene Ther* 1999; **10**: 1349–1358.
16. Eto Y, Gao JQ, Sekiguchi F, *et al.* Neutralizing antibody evasion ability of adenovirus vector induced by the bioconjugation of MPEG-SPA. *Biol Pharm Bull* 2004; **27**: 936–938.
17. Alemany R, Suzuki K, Curiel DT. Blood clearance rates of adenovirus type 5 in mice. *J Gen Virol* 2000; **81**: 2605–2609.
18. Lanciotti J, Song A, Doukas J, *et al.* Targeting adenoviral vectors using heterofunctional polyethylene glycol FGF2 conjugates. *Mol Ther.* 2003; **8**: 99–107.
19. Ogawara K, Rots MG, Kok RJ, *et al.* A novel strategy to modify adenovirus tropism and enhance transgene delivery to activated vascular endothelial cells in vitro and in vivo. *Hum Gene Ther* 2004; **15**: 433–443.
20. Bergelson JM, Krithivas A, Celi L, *et al.* The murine CAR homolog is a receptor for coxsackie B viruses and adenoviruses. *J Virol* 1998; **72**: 415–419.
21. Tomko RP, Xu R, Philipson L. HCAR and MCAR: the human and mouse cellular receptors for subgroup C adenoviruses and group B coxsackieviruses. *Proc Natl Acad Sci U S A* 1997; **94**: 3352–3356.
22. Bewley MC, Springer K, Zhang YB, *et al.* Structural analysis of the mechanism of adenovirus binding to its human cellular receptor, CAR. *Science* 1999; **286**: 1579–1583.
23. Wickham TJ, Mathias P, Cheresh DA, Nemerow GR. Integrins alpha v beta 3 and alpha v beta 5 promote adenovirus internalization but not virus attachment. *Cell* 1993; **73**: 309–319.
24. Mathias P, Wickham T, Moore M, Nemerow G. Multiple adenovirus serotypes use alpha v integrins for infection. *J Virol* 1994; **68**: 6811–6814.
25. Koizumi N, Mizuguchi H, Hosono T, *et al.* Efficient gene transfer by fiber-mutant adenoviral vectors containing RGD peptide. *Biochim Biophys Acta* 2001; **1568**: 13–20.
26. Reynolds P, Dmitriev I, Curiel D. Insertion of an RGD motif into the HI loop of adenovirus fiber protein alters the distribution of transgene expression of the systemically administered vector. *Gene Ther* 1999; **6**: 1336–1339.
27. Mizuguchi H, Kay MA. Efficient construction of a recombinant adenovirus vector by an improved in vitro ligation method. *Hum Gene Ther* 1998; **9**: 2577–2583.
28. Maizel JV Jr, White DO, Scharff MD. The polypeptides of adenovirus. I. Evidence for multiple protein components in the

virion and a comparison of types 2, 7A, and 12. *Virology* 1968; **36**: 115–125.
29. Rink H. Solid-phase synthesis of protected peptide fragments using a trialkoxydiphenylmethyl ester resin. *Tetrahedron Lett* 1987; **28**: 3787–3790.
30. Sieber P. Modification of tryptophan residues during acidolysis of 4-methoxy-2,3,6-trimethylbenzenesulfonyl groups. *Tetrahedron Lett* 1987; **28**: 1637–1641.
31. Chillon M, Lee JH, Fasbender A, *et al.* Adenovirus complexed with polyethylene glycol and cationic lipid is shielded from neutralizing antibodies in vitro. *Gene Ther* 1998; **5**: 995–1002.
32. Xu ZL, Mizuguchi H, Ishii-Watabe A, *et al.* Optimization of transcriptional regulatory elements for constructing plasmid vectors. *Gene* 2001; **11**: 149–156.
33. Wu ZZ, Li P, Huang QP, *et al.* Inhibition of adhesion of hepatocellular carcinoma cells to basement membrane components by receptor competition with RGD- or YIGSR-containing synthetic peptides. *Biorheology* 2003; **40**: 489–502.
34. Bronson RA, Fusi F. Evidence that an Arg-Gly-Asp adhesion sequence plays a role in mammalian fertilization. *Biol Reprod* 1990; **43**: 1019–1025.
35. Hardy S, Kitamura M, Harris-Stansil T, *et al.* Construction of adenovirus vectors through Cre-lox recombination. *J Virol* 1997; **71**: 1842–1849.
36. Von Seggern DJ, Chiu CY, Fleck SK, *et al.* A helper-independent adenovirus vector with E1, E3, and fiber deleted: structure and infectivity of fiberless particles. *J Virol* 1999; **73**: 1601–1608.
37. Zou L, Zhou H, Pastore L, Yang K. Prolonged transgene expression mediated by a helper-dependent adenoviral vector (hdAd) in the central nervous system. *Mol Ther* 2000; **2**: 105–113.
38. Belousova N, Krendelchtchikova V, Curiel DT, Krasnykh V. Modulation of adenovirus vector tropism via incorporation of polypeptide ligands into the fiber protein. *J Virol* 2002; **76**: 8621–8631.
39. Nicklin SA, Von Seggern DJ, Work LM, *et al.* Ablating adenovirus type 5 fiber-CAR binding and HI loop insertion of the SIGYPLP peptide generate an endothelial cell-selective adenovirus. *Mol Ther* 2001; **4**: 534–542.

Available online at www.sciencedirect.com

SCIENCE DIRECT®

Journal of Controlled Release 105 (2005) 344–353

journal of controlled release

www.elsevier.com/locate/jconrel

Fusogenic liposome delivers encapsulated nanoparticles for cytosolic controlled gene release

Jun Kunisawa[a,1], Takashi Masuda[a,1], Kazufumi Katayama[a], Tomoaki Yoshikawa[a,b], Yasuo Tsutsumi[a,b], Mitsuru Akashi[b,c], Tadanori Mayumi[a], Shinsaku Nakagawa[a,b,*]

[a]*Department of Biopharmaceutics, Graduate School of Pharmaceutical Sciences, Osaka University 1-6 Yamadaoka, Suita, Osaka 565-0871, Japan*

[b]*"Creation of bio-devices and bio-systems with chemical and biological molecules for medical use", CREST, Japan Science and Technology Corporation (JST), Japan*

[c]*Department of Nanostructured and Advanced Materials, Graduate School of Science and Engineering, Kagoshima University, Japan*

Received 8 December 2004; accepted 18 March 2005
Available online 3 June 2005

Abstract

Therapeutic agents based on DNA or RNA oligonucleotides (e.g., antisense DNA oligonucleotide, small interfering RNA) require a regulation of their kinetics in cytoplasm to maintain an optimal concentration during the treatment period. In this respect, delivery of functional nanoparticles containing these drugs into cytoplasm has been thought to have a potential for the cytosolic controlled gene release. In this study, we establish a protocol for the encapsulation of nanoparticles into liposome, which is further fused with ultra violet-inactivated Sendai virus to compose fusogenic liposomes. When nanoparticles were encapsulated in conventional liposomes, endocytosis-mediated uptake of nanoparticles was observed. In contrast, numerous amounts of nanoparticles were delivered into the cytoplasm without any cytotoxicity when the particles were encapsulated in fusogenic liposomes. Additionally, fusogenic liposome showed a high ability to deliver nanoparticles containing DNA oligonucleotides into cytoplasm. These results indicate that this combinatorial nanotechnology using fusogenic liposome and nanoparticle is a valuable system for regulating the intracellular pharmacokinetics of gene-based drugs.

Keywords: Fusogenic liposome; Nanoparticle; Nanotechnology; Drug delivery; Antisense oligonucleotide DNA

1. Introduction

Among recent advances in nanotechnology, one of the most prominent progresses is its application to drug delivery. Numerous drug carriers with nano-scale sizes like a nanoparticle (NP), liposome, dendrimer and nanocrystal have been developed and some of

* Corresponding author. Department of Biopharmaceutics, Graduate School of Pharmaceutical Sciences, Osaka University 1-6 Yamadaoka, Suita, Osaka 565-0871, Japan. Tel./fax: +81 6 6879 8176.
E-mail address: nakagawa@phs.osaka-u.ac.jp (S. Nakagawa).
[1] These authors contributed equally to the work.

0168-3659/$ - see front matter © 2005 Elsevier B.V. All rights reserved.
doi:10.1016/j.jconrel.2005.03.020

them are already in clinical use [1–3]. The major aim of these delivery systems is to regulate "systemic pharmacokinetics" such as drug absorption, distribution (e.g., tissue-specific targeting), metabolism and elimination in vivo [4,5]. However, recent advancements on drug design have proposed that the regulation of "intracellular pharmacokinetics" is also important for drugs targeting intracellular components [6,7].

Novel gene-based therapies using an antisense DNA and small interference RNA (siRNA) represent an enormously promising approach to decrease or modulate an expression of their target molecules [7–11]. Since the main physiological target of these drugs is messenger RNA, it is pivotal to deliver them into cytoplasm. Although there are systems, including ours, that can achieve the delivery of soluble drugs into cytoplasm [12–15], a novel delivery system to introduce NPs containing gene-based drugs into cytoplasm will provide further advantages for the maintenance of the optimal concentration by protecting the genes from hydrolytic and enzymatic degradation.

We previously developed fusogenic liposome (FL) having Sendai virus envelope glycoproteins on the surface and reported that FL could efficiently introduce encapsulated nucleotides and/or proteins into the cytoplasm through its direct fusion to the plasma membrane without cytotoxicity [12,16]. We also demonstrated an application of FL to gene therapy, cancer chemotherapy and vaccine development [17–22]. These progressive results lead us to suppose that FL would also be able to transport NP into the cytoplasm if NP would be encapsulated in FL. In the present study, we determine an optimal protocol to encapsulate a NP into conventional liposome (Lipo) and to fuse them subsequently with Sendai virus to formulate FL. We also present that FL shows a high ability to introduce the encapsulated NPs into cytoplasm, which is applicable to cytosolic controlled gene release.

2. Materials and methods

2.1. Preparation of FL encapsulating NP

Lipo was prepared by a dehydration–rehydration method [23]. Briefly, a lipid mixture, composed of phosphatidylcholine, L-α-dimyristoyl phosphatidic acid, and cholesterol (NOF Corporation, Tokyo, Japan) in a 4:5:1 molar ratio, was suspended in solution containing chloroform, methanol and water (65:25:4) and evaporated to remove chloroform and methanol. To label liposomal membrane with rhodamine, rhodamine-labeled diacylphosphatidyl ethanolamine (Molecular Probes, Eugene, OR) was added to the mixture. The lipid mixture was further frozen in liquid nitrogen and lyophilized overnight. The resulting lipid powder was hydrated with solution containing FITC-labeled NP (Molecular Probes) or oligonucleotide-adsorbed NP (about $0.5–3 \times 10^{11}$ particles/ml). Conventional liposome (Lipo) was prepared from the hydrated mixture by a hand-held extruder with two layers of cellulose acetate membranes (pore size, 800 nm in diameter) (Advantec, Osaka, Japan) and washed with phosphate-buffered saline (PBS).

For preparation of FL, NP encapsulated in Lipo (NP–Lipo) was mixed with UV-inactivated Sendai virus and incubated with vigorous shaking for 2 h at 37 °C. FL was finally purified by stepwise sucrose-density centrifugation (77,000 $\times g$, 2 h, 4 °C) as described previously [16].

2.2. Preparation of poly (vinyl amine) NP

Preparation of poly (vinyl amine) NP was described previously [24]. Briefly, poly (vinyl acetamide) macromer was prepared from monomers by free radical polymerization, in which 2,2′-azobisisobutyronitrile (AIBN) and 2-mercaptoethanol were used as an initiator and a chain transfer agent, respectively, and then *p*-chloromethyl styrene was used to introduce a vinyl benzyl group. Nonionic poly (vinyl acetamide) NP was produced by copolymerization between the macromonomers and styrene after initiation with AIBN. Surface cationized poly (vinyl amine) NP was prepared by hydrolyzing poly (vinyl acetamide) NP in 4 N HCl at 80 °C. The resulting poly (vinyl amine) NP was dialyzed to remove unreacted substances and then was lyophilized.

To prepare oligonucleotide-adsorbed NP, poly (vinyl amine) NP (6×10^{10} particles/ml) was mixed with FITC-labeled phosphorothioate oligo deoxynucleotides (GCCCAAGCTGGCATCCGTCA, 3×10^{15} copies/ml, Geneset, Kyoto, Japan) for 1 h at room temperature.

2.3. Transmission electron microscopy (TEM)

To visually examine liposome structure, Cryo-TEM was employed. Specimens were prepared by depositing a small droplet of liposome suspension on a TEM grid coated with poly-lysine, vitrified by plunging it into liquid ethane, and observed by TEM (TECNAI F20TWIN; Phillips, Mahwah, NJ).

For the analysis of intracellular distribution of NP, LLCMK2 cells cultured on collagen-coated plates were treated with NP–FL for 30 min. After washing three times with PBS, the cells were fixed with 2% glutaraldehyde for 2 h at 4 °C and then post-fixed with 1% osmium tetroxide for 2 h at 4 °C. After dehydration by immersing in serially diluted aqueous ethanol solutions, the specimens were embedded in epoxy resin, sectioned to 80–100 nm thick, stained with uranyl acetate, and examined by TEM.

2.4. Confocal microscopy and flow cytometry

LLCMK2, HeLa, HL-60, HUVEC or DC2.4 cells (kindly gifted from Dr. K. Rock, University of Massachusetts Medical School) (10^5 cells/well) were plated in a 24-well plate and were cultured overnight for subsequent experiments. To measure NP delivery, the cells were treated with NP-alone, NP–Lipo, or NP–FL (300 particles/cell) for 30 min, washed, and observed by confocal microscopy (Bio-Rad, Hercules, CA). Simultaneously, nucleus was stained with 1 mM SYTO64 (Molecular Probes).

The treated cells were also dissociated from plates by treating with 0.25% trypsin and were analyzed by FACScan flow cytometer (Becton Dickinson, Mansfield, MA). To inhibit endocytosis, LLCMK2 cells were treated with 5 μg/ml of cytochalasin B or 0.2 μg/ml of cytochalasin D (Sigma, St Louis, MO). Following 1-h incubation, NP–Lipo (3000 particles/cell) or NP–FL (300 particles/cell) were added and the cells were cultured for 30 min. Uptake efficiency was measured by flow cytometry.

2.5. Cytotoxic assay

To assess the cytotoxicity of NP-alone, NP–Lipo or NP–FL, LLCMK2 cells were treated with the particles (300 particles/cell) for 30 min. Following three times washing with PBS, the cells were split into 96-well plate (5×10^2 cells/well) and cultured for 1, 2, 4, or 6 days. The cell viability was determined by 3-(4,5-dimethylthiazol-2-yl)-2,5-diphenyl tetrazolium bromide (MTT).

3. Results and discussion

3.1. Development and characterization of FL containing NP

We firstly evaluated the encapsulation of NP into Lipo using fluorescein isothiocyanate (FITC)-labeled NP (500 nm in diameter) and rhodamine-labeled Lipo. The different densities of empty Lipo ($d = 1.02$) and NP ($d = 1.12$) allowed us to discriminate them by sucrose-density gradient centrifugation. Fluorescence activity derived from empty Lipo and that from NP were detected in fractions 2–3 and fractions 14–15, respectively (Fig. 1A). We also found intermediate fractions (fractions 8–11) exhibiting both NP-derived FITC and Lipo-derived rhodamine fluorescence, which suggested that these fractions contained NP encapsulated in or attached with Lipo (Fig. 1A). To elucidate whether NP was attached with or encapsulated in Lipo, we performed cryo-transmission electron microscopy (Cryo-TEM). This analysis clarified that NP-alone was detected in fractions 14–15 (Fig. 1B) and that NP in fractions 8–11 was surrounded with lipid membrane, indicating that intermediate fractions contained NP encapsulated in Lipo (Fig. 1C).

NP encapsulated in Lipo (NP–Lipo) was then incubated with ultraviolet-inactivated Sendai virus in order to make NP encapsulated in FL (NP–FL). To evaluate the formulation of NP–FL, we mixed fluorescence labeled NP–Lipo with ultraviolet-inactivated Sendai virus followed by analyzing the fluorescence activity after stepwise sucrose-density gradient centrifugation (10%, 30% and 50%). The gradient centrifugation of the mixture resulted in two distinct peaks (Fig. 1D). Cryo-TEM analysis indicated that fractions 8–9 are successfully identical to NP–FL because lipid membrane in the fractions exhibited a spiked structure of envelope proteins derived from Sendai virus (Fig. 1E and F). This conclusion was further confirmed by their diameter and zeta potential at the surface. The diameter of NP–FL (880 nm) is bigger than that of NP–Lipo (750 nm) and

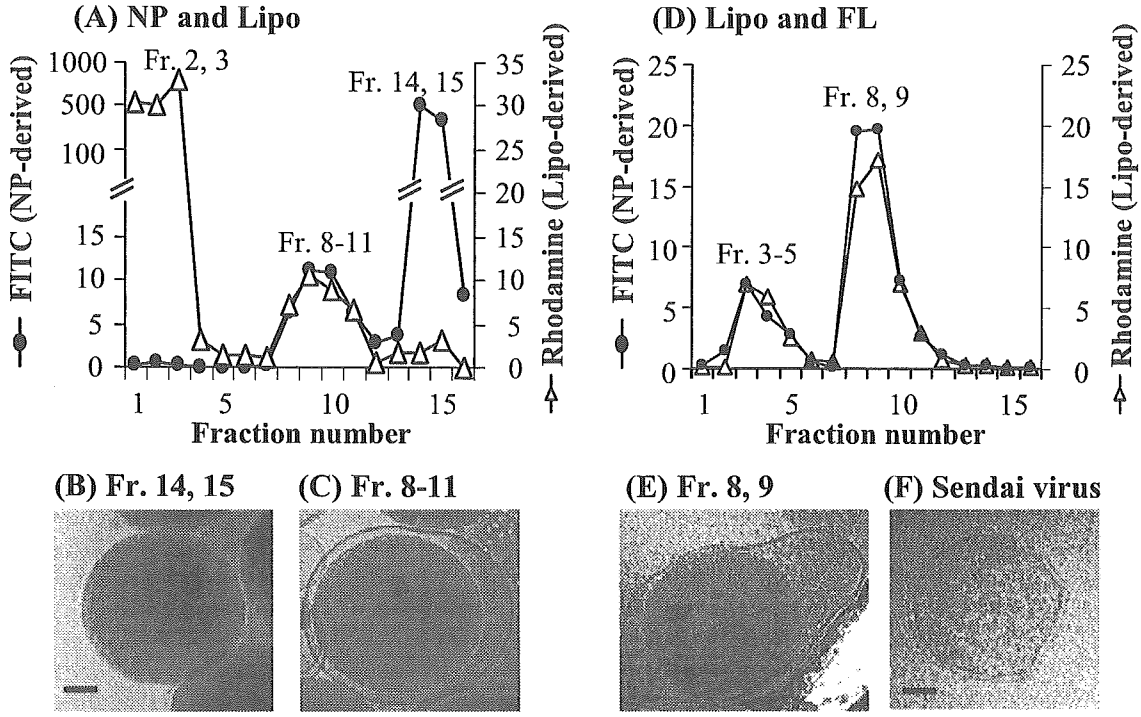

Fig. 1. Characterization of NP–Lipo and NP–FL. (A) FITC-labeled NP was encapsulated in rhodamine-labeled Lipo. After stepwise fractionation through sucrose-density centrifugation (6%, 10% and 30%), fluorescent intensity derived from FITC-NP (closed circle) or rhodamine-Lipo (open triangle) was measured. (B and C) Fractions 14–15 in A (B, NP-alone) or fractions 8–11 in A (C, NP–Lipo) were visualized by Cryo-TEM. Bar corresponds to 100-nm length. (D) NP–FL was prepared by fusing ultraviolet-inactivated Sendai virus with NP–Lipo. The resultant was purified by stepwise sucrose-density centrifugation (10%, 30% and 50%) and fluorescent intensity of each fraction was analyzed as described in A. (E and F) Fractions 8–9 in D (E, NP–FL) or ultraviolet-inactivated Sendai virus (F) were observed by Cryo-TEM. Bar is identical to 100 nm.

of Sendai virus (300 nm). Additionally, surface zeta-potential of fractions 8–9 (−15 mV) was largely different from that of NP–Lipo (−27 mV) because they were affected by the different electronic charge of Sendai virus (−13 mV).

In this study, we used 500 nm NP in diameter. In addition, we also successfully encapsulated 20 nm or 100 nm NP in Lipo as well as FL with equal efficiency (only data using 500 nm NP are shown in this study). Further, we are also capable of regulating the liposomal size by selection of the membrane pore size for the extrusion (the average size of NP–FL used in this study is 880 nm in diameter). Also we can regulate surface electronic characteristics of FL membrane by selecting the lipid composition. These results suggest that the protocol described in this study is a versatile system to encapsulate various sizes of NP into FL with various characteristics.

3.2. Efficient delivery of NP by FL

To examine the feasibility of Lipo and FL as a vehicle to deliver NP, LLCMK2 cells were incubated with FITC-labeled NP encapsulated in either Lipo or FL and were observed by confocal microscopy. In spite of the fact that only a few NPs were observed in the cells incubated with NP-alone or NP–Lipo (Fig. 2A and B), a large number of NPs were detected when the cells were treated with NP–FL (Fig. 2C and D). Simultaneous staining of nucleus with SYTO64 indicated that 500 nm NP was not noticed at the nucleus (Fig. 2C and D). This is a predictable observation because nuclear pore complex can transport a particle within 40 nm in diameter [25].

As a next experiment, flow cytometry analysis was employed to evaluate the efficiency of FL for delivery of the encapsulated NP. Several fluorescent peaks

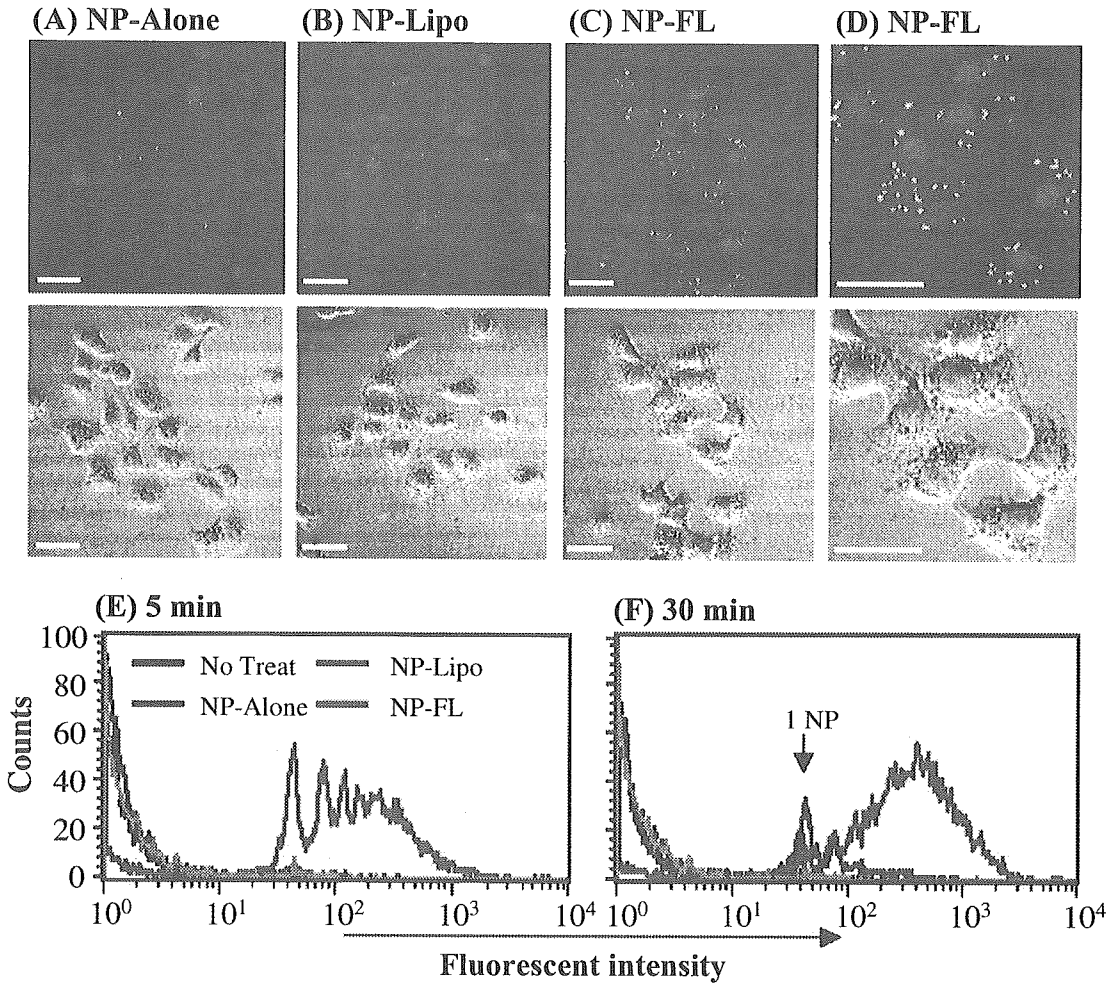

Fig. 2. FL-mediated effective delivery of NP. (A–D) LLCMK2 cells were incubated with FITC-labeled NP without encapsulation (A, NP-alone) or encapsulated in either Lipo (B, NP–Lipo) or FL (C and D, NP–FL) for 30 min. After staining of nucleus with SYTO 64 (red), the cells were observed by confocal microscopy (top). The same specimens were visualized by transmission microscopy (bottom). Bars indicate 50 μm at ×400 (A–C) or ×800 (D) magnification. (E and F) LLCMK2 cells were incubated with NP-alone (green), NP–Lipo (blue), or NP–FL (red) for 5 min (E) or 30 min (F). Fluorescence originated from FITC-labeled NP was measured by a FACScan flow cytometer.

were observed 5 min after the treatment of the cells with NP–FL, whereas fluorescence was barely detectable when the cells were incubated with NP-alone or NP–Lipo (Fig. 2E). This is consistent with our previous result that delivery by FL is mediated by membrane fusion but not by endocytosis, which is faster and more efficient than that of endocytosis-mediated Lipo uptake [16]. Thus, we could detect fluorescence intensity of the cells treated with NP–Lipo after 30 min incubation (Fig. 2F), implying that this uptake might occur through endocytosis. It should be noted that a fluorescence intensity of the cells treated with NP–FL was still much higher than that of the cells incubated with NP-alone or with NP–Lipo after 30-min incubation (Fig. 2F). These results suggested that FL could deliver the encapsulated NPs into the cells in an effective and fast manner.

To show quantitative data for the effective NP delivery, the number of NPs incorporated into a cell after 30-min incubation was calculated by the mean fluorescence intensity of 40 per NP in a cell (arrow, Fig. 2F). Consistent with the results of confocal

Table 1
The number of NPs incorporated in 1 cell was calculated by the result that cells containing 1 NP presented 40 of mean fluorescence intensity after 30 min incubation as described in Fig. 2F

Number	NP-alone	NP–Lipo	NP–FL
0	97.8 ± 0.67	85.8 ± 0.92	5.8 ± 0.38
1–5	2.1 ± 0.06	13.7 ± 0.79	29.9 ± 2.76
6–10	0.1 ± 0.01	0.5 ± 0.13	31.2 ± 1.19
11–25	Undetectable	0.1 ± 0.03	28.9 ± 2.01
26–more	Undetectable	Undetectable	5.3 ± 1.58

Results are expressed as the means ± SE from three independent experiments.

microscopy, NPs were not detected in most cells (97.8%) incubated with NP-alone (Table 1). Similarly, only 1–5 NPs were observed in about 15% of cells incubated with NP–Lipo (Table 1). Conversely, about 95% of cells incubated with NP–FL had detectable NP, with approximately ten NPs per cell on average. Furthermore, about 5% cells contained more than 26 NPs with strong fluorescence intensity (Table 1 and Fig. 2F). These results further emphasize the effectiveness of FL for NP delivery into the cells.

We next investigated the FL-mediated NP delivery into several cell lines to address the specificity. Similar efficiency was determined when NP–FL was incubated with human-derived adherent (HeLa), non-adherent (HL60), and primary culture (HUVEC) cells, while these cells could not take NP-alone or NP–Lipo effectively (Fig. 3A–C). However, murine dendritic cell lines (DC2.4) showed slightly higher uptake activity for NP-alone or NP–Lipo (Fig. 3D). This is due to a high endo-phagocytosis ability of dendritic cell that is well known as an antigen sampling and presenting cells [26]. It should be noted

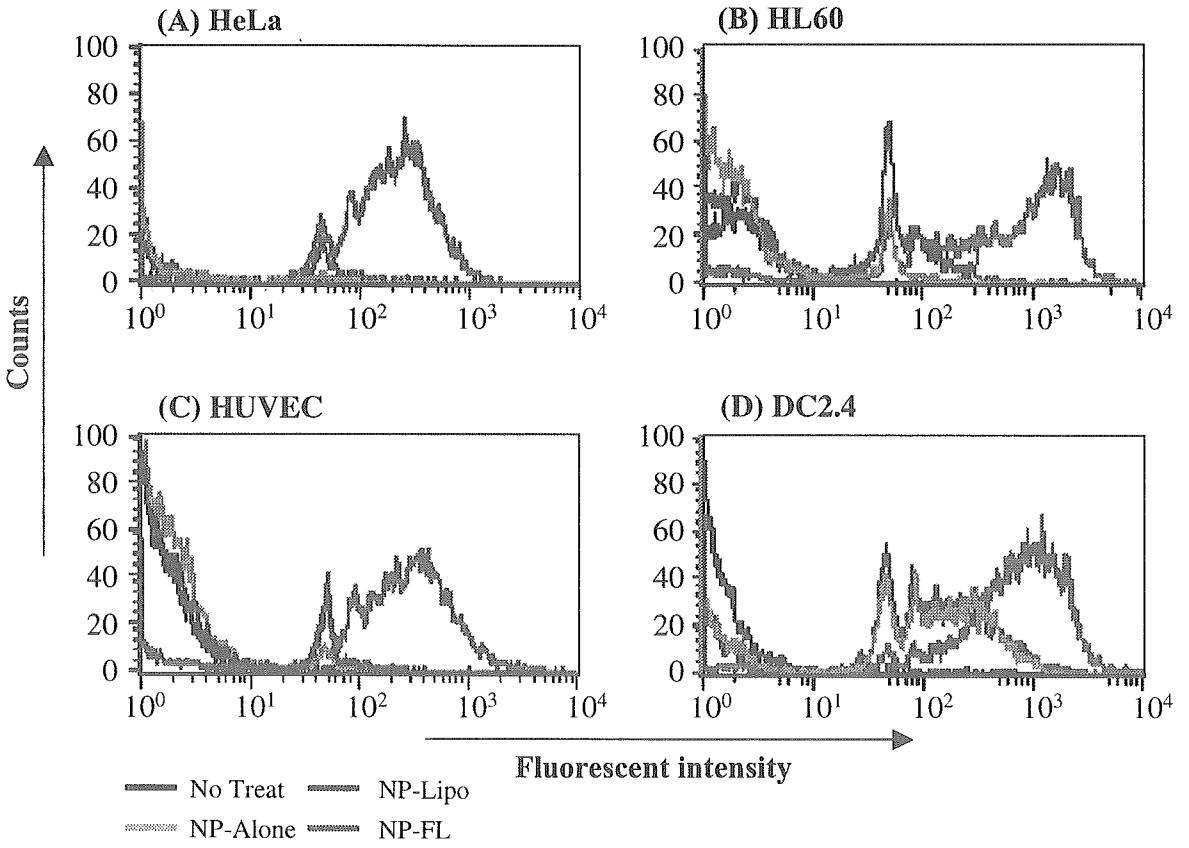

Fig. 3. FL effectively delivers the encapsulated NPs into various kinds of cells. HeLa cells (A), HL60 cells (B), HUVEC (C), or DC2.4 cells (D) were treated with none (black), NP-alone (green), NP–Lipo (blue), or NP–FL (red) for 30 min. Fluorescent intensity in the cell derived from FITC-labeled NP was measured by a FACScan flow cytometer.

again that the number of NPs delivered by FL is still much higher than that of Lipo and the efficiency was not altered in the cells showing high endocytosis activity (Fig. 3D). This observation convinced us that FL-mediated high efficient NP delivery was independent on endocytosis activity. In our previous study, the delivery to a wide variety of cells by FL was also determined and seemed to depend on indiscriminative fusion activity of Sendai virus [27].

3.3. Endocytosis-independent NP delivery into cytoplasm by FL

As mentioned above, FL can efficiently deliver the encapsulated contents to the cytoplasm through its direct fusion with the plasma membrane [16]. Thus, we next tried to test whether NP delivery by FL was also mediated through membrane fusion, rather than through endocytosis. To address this, cells were treated with an endocytosis inhibitor, cytochalasin B or cytochalasin D, followed by the addition of NP–FL or NP–Lipo. While cytochalasin B treatment resulted in a marked reduction of NP–Lipo uptake, no inhibition of NP uptake was observed when cells were incubated with NP–FL (Fig. 4A). Similar results were obtained when cells were treated with the other inhibitors, cytochalasin D (Fig. 4A), 2,4-dinitrophenol, nocodazole or colchicine (data not shown). These results indicated that FL could deliver the encapsulated NPs into the cytoplasm by membrane fusion, rather than by endocytosis. Based on these data, we supposed that NPs delivered by FL was located in cytoplasm, not in endosome. To prove this speculation, TEM analysis was performed to show visually the distribution of NP introduced by FL. The histological analysis showed that NPs existed in the cytoplasm, not in the endosome, of cells treated with NP–FL (Fig. 4B and C).

Most of drug-delivery vehicles, including conventional liposome, enter into cells via endocytosis and then are delivered to lysosomes, where they as well as their contents are degraded [28,29]. Thus, drugs delivered by NP-alone or NP–Lipo are likely degraded in lysosome even if these vehicles are taken up. In contrast, NP–FL can deliver NP efficiently to the cytoplasm not via endocytosis (Figs. 2–4, Table 1). These findings indicated that FL had a benefit not only to deliver the numerous numbers of NP but also to deliver the contents into cytoplasm without their

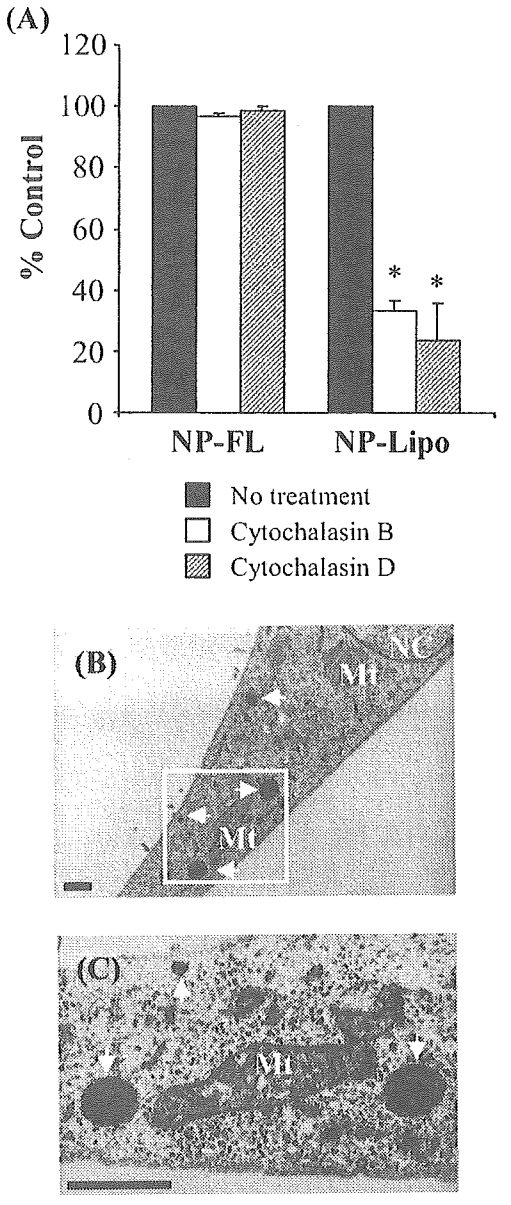

Fig. 4. Endocytosis-independent NP delivery into cytoplasm by FL. (A) LLCMK2 cells were not pre-treated (solid) and pre-treated with 5 μg/ml cytochalasin B (open) or 0.2 μg/ml cytochalasin D (slashed) for 1 h and incubated with NP–FL or NP–Lipo for additional 30 min. Then, the number of FITC-NP positive cells was analyzed by FACScan flow cytometry. Error bars indicate the means ± SE of three independent experiments. (B) LLCMK2 cells were cultured with NP–FL for 30 min and observed by Cryo-TEM. Mitochondrion and nucleus are marked with 'Mt' and 'NC', respectively. Arrowheads indicate NPs. Bars are 1 μm at ×7000 (B) or ×20,000 (D) magnification.

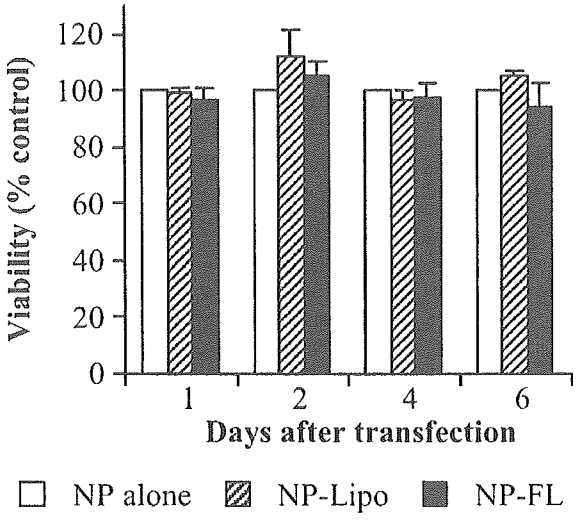

Fig. 5. Toxicity of NP-alone, NP–Lipo, or NP–FL. The NP-alone (open), NP–Lipo (hatched), and NP–FL (closed) were incubated with LLCMK2 cells for 30 min. Following washing with PBS, the cells were cultured for 1, 2, 4, and 6 days. MTT assay was performed to determine the cell viability.

degradation in endosome/lysosome pathway. Furthermore, MTT assay revealed that NP–FL did not show any cytotoxicity against target cells for at least one week after the transfection (Fig. 5).

In this study, we used non-degradable NPs as a model NP. The experimental restriction in cell culture made it difficult to determine the fate of the NPs after the long culture. One possible hypothetical pathway is that NP is excluded to extracellular compartments by exocytosis pathway and/or cell death. Since the non-degradable NPs are difficult to be applied to in vivo use, our current study to expand this technology to biodegradable NPs (e.g., poly lactic acid NPs) is ongoing. Nevertheless, this study allows us to propose that the FL technology has the following advantages over other vehicles: efficient delivery of its contents to the cytoplasm of a wide range of target cells, lack of cytotoxicity, and ease of encapsulation of various NPs.

3.4. Controlled release of DNA oligonucleotides from NP in cytoplasm

To show a potential application of NP–FL system for gene delivery, we examined delivery of DNA oligonucleotides by NP–FL. FITC-labeled phosphorothioate oligonucleotides were immobilized on poly (vinyl amine) NP and were encapsulated into FL. Similar to the above observations (Figs. 2 and 3), flow cytometry analysis demonstrated that delivery efficiency of NP–FL was superior to that of NP–Lipo or NP-alone (Fig. 6). Inhibitor experiments also convinced us that the FL-mediated NP delivery depended on fusion activity of FL (data not shown).

We used in this study single type of NP for gene delivery experiment. Progresses on particle technology in the last decade allow us to select NPs exhibiting a different drug release profile by their characteristics (e.g., surface electron characteristics, hydrophile–lipophile balance) [30–32]. Since FL can encapsulate and deliver various kinds of NP into cells, NPs with different drug release profiles can be introduced into a cell, which may present the "timing drug release". This system is now under investigation. In addition to the modification of encapsulated NPs, our present effort is aimed to demonstrate the feasibility of FL-mediated NP delivery for gene therapy using bioactive DNA and/or RNA oligonucleotides (e.g., RNA interference).

Some groups have already demonstrated the cytosolic particle delivery. Panyam et al. reported that poly (DL-lactide-co-glycolide) NPs were delivered into cytosol by endo-lysosomal escape mechanism [33]. Although they showed an application of that

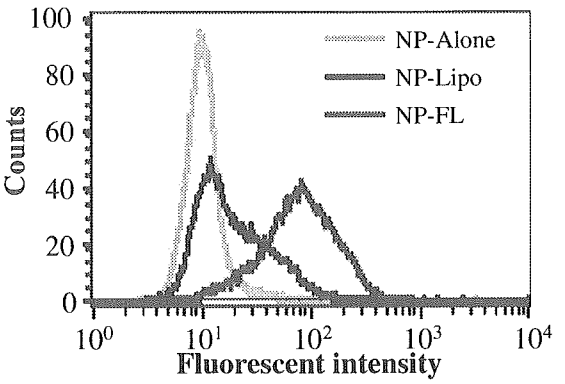

Fig. 6. Efficient delivery of NP containing DNA oligonucleotides into cytoplasm by FL. LLCMK2 cells were cultured with oligonucleotide-immobilized NPs without encapsulation (green) or encapsulated in either Lipo (blue) or FL (red) for 30 min. Fluorescent intensity of the cells were analyzed by a FACScan flow cytometer.

system to intracellular drug release (e.g., dexamethasone and plasmid) from the NPs, we can assert that our NP delivery system is more efficient than their system because the efficacy of FL-mediated NP delivery was much higher than that of endocytosis-mediated uptake even in dendritic cells having a high ability to do endocytosis or phagocytosis (Fig. 3D). In the other approach, HIV-derived TAT peptide was employed for cytoplasmic NP delivery. It was demonstrated that TAT peptide-attached liposome was delivered into cells [34]. Additionally, the group also illustrated the application of TAT-attached liposome to DNA delivery in vitro and in vivo [35]. This is an interesting approach, but they have not unfortunately been succeeded in sustained drug release because the liposome was degraded quickly (within 24 h). Thus, we emphasize that this study demonstrated for the first time that NP is delivered by FL into cytoplasm for the possible application to sustained gene release.

4. Conclusion

In conclusion, we establish a protocol to encapsulate NP into FL and demonstrate that FL is an effective delivery vehicle to introduce the encapsulated NP into cytoplasm. We propose here that the combinatorial nanotechnology, NP–FL, will provide an opportunity for the kinetics regulation of genetic drugs in the cytoplasm.

Acknowledgments

We are grateful to Mr. M. Mori and Mr. K. Sakaguchi at NOF Corporation for supplying us with lipid mixture. We also acknowledge Mr. T. Watanabe at FEI Company for his technical assistance on an electron microscopy study and Dr. Susan Schwab for careful reading of the manuscript. This study was supported in part by Core Research for the Evolutional Science and Technology Program, Japan Science and Technology Corp. and by Grant-in-Aid for Scientific Research (B) from the Ministry of Education, Culture, Sports, Science, and Technology of Japan. J. Kunisawa is a research fellow of the Japan Society for the Promotion of Science.

References

[1] D.A. LaVan, D.M. Lynn, R. Langer, Moving smaller in drug discovery and delivery, Nat. Rev. Drug Discov. 1 (1) (2002) 77–84.
[2] R. Duncan, The dawning era of polymer therapeutics, Nat. Rev. Drug Discov. 2 (5) (2003) 347–360.
[3] H. Otsuka, Y. Nagasaki, K. Kataoka, PEGylated nanoparticles for biological and pharmaceutical applications, Adv. Drug Deliv. Rev. 55 (3) (2003) 403–419.
[4] R.M. Schek, S.J. Hollister, P.H. Krebsbach, Delivery and protection of adenoviruses using biocompatible hydrogels for localized gene therapy, Molec. Ther. 9 (1) (2004) 130–138.
[5] M.E. Akerman, W.C. Chan, P. Laakkonen, S.N. Bhatia, E. Ruoslahti, Nanocrystal targeting in vivo, Proc. Natl. Acad. Sci. U. S. A. 99 (20) (2002) 12617–12621.
[6] J. Alper, Drug delivery. Breaching the membrane, Science 296 (5569) (2002) 838–839.
[7] J.B. Opalinska, A.M. Gewirtz, Nucleic-acid therapeutics: basic principles and recent applications, Nat. Rev. Drug Discov. 1 (7) (2002) 503–514.
[8] Y.S. Cho-Chung, Antisense DNAs as targeted genetic medicine to treat cancer, Arch. Pharm. Res. 26 (3) (2003) 183–191.
[9] T. Suwanmanee, H. Sierakowska, S. Fucharoen, R. Kole, Repair of a splicing defect in erythroid cells from patients with beta-thalassemia/HbE disorder, Molec. Ther. 6 (6) (2002) 718–726.
[10] N.R. Wall, Y. Shi, Small RNA: can RNA interference be exploited for therapy? Lancet 362 (9393) (2003) 1401–1403.
[11] E. Song, S.K. Lee, J. Wang, N. Ince, N. Ouyang, J. Min, J. Chen, P. Shankar, J. Lieberman, RNA interference targeting Fas protects mice from fulminant hepatitis, Nat. Med. 9 (3) (2003) 347–351.
[12] J. Kunisawa, S. Nakagawa, T. Mayumi, Pharmacotherapy by intracellular delivery of drugs using fusogenic liposomes: application to vaccine development, Adv. Drug Deliv. Rev. 52 (3) (2001) 177–186.
[13] N. Murthy, M. Xu, S. Schuck, J. Kunisawa, N. Shastri, J.M. Frechet, A macromolecular delivery vehicle for protein-based vaccines: acid-degradable protein-loaded microgels, Proc. Natl. Acad. Sci. U. S. A. 100 (9) (2003) 4995–5000.
[14] M.C. Morris, J. Depollier, J. Mery, F. Heitz, G. Divita, A peptide carrier for the delivery of biologically active proteins into mammalian cells, Nat. Biotechnol. 19 (12) (2001) 1173–1176.
[15] E. Mathew, G.E. Hardee, C.F. Bennett, K.D. Lee, Cytosolic delivery of antisense oligonucleotides by listeriolysin O-containing liposomes, Gene Ther. 10 (13) (2003) 1105–1115.
[16] H. Mizuguchi, T. Nakagawa, M. Nakanishi, S. Imazu, S. Nakagawa, T. Mayumi, Efficient gene transfer into mammalian cells using fusogenic liposome, Biochem. Biophys. Res. Commun. 218 (1) (1996) 402–407.
[17] H. Mizuguchi, T. Nakagawa, S. Toyosawa, M. Nakanishi, S. Imazu, T. Nakanishi, Y. Tsutsumi, S. Nakagawa, T. Hayakawa, N. Ijuhin, T. Mayumi, Tumor necrosis factor alpha-mediated tumor regression by the in vivo transfer of genes into the artery that leads to tumors, Cancer Res. 58 (24) (1998) 5725–5730.

[18] H. Mizuguchi, M. Nakanishi, T. Nakanishi, T. Nakagawa, S. Nakagawa, T. Mayumi, Application of fusogenic liposomes containing fragment A of diphtheria toxin to cancer therapy, Br. J. Cancer 73 (4) (1996) 472–476.

[19] T. Nakanishi, A. Hayashi, J. Kunisawa, Y. Tsutsumi, K. Tanaka, Y. Yashiro-Ohtani, M. Nakanishi, H. Fujiwara, T. Hamaoka, T. Mayumi, Fusogenic liposomes efficiently deliver exogenous antigen through the cytoplasm into the MHC class I processing pathway, Eur. J. Immunol. 30 (6) (2000) 1740–1747.

[20] A. Hayashi, T. Nakanishi, J. Kunisawa, M. Kondoh, S. Imazu, Y. Tsutsumi, K. Tanaka, H. Fujiwara, T. Hamaoka, T. Mayumi, A novel vaccine delivery system using immunopotentiating fusogenic liposomes, Biochem. Biophys. Res. Commun. 261 (3) (1999) 824–828.

[21] J. Kunisawa, T. Nakanishi, I. Takahashi, A. Okudaira, Y. Tsutsumi, K. Katayama, S. Nakagawa, H. Kiyono, T. Mayumi, Sendai virus fusion protein mediates simultaneous induction of MHC class I/II-dependent mucosal and systemic immune responses via the nasopharyngeal-associated lymphoreticular tissue immune system, J. Immunol. 167 (3) (2001) 1406–1412.

[22] G. Sakaue, T. Hiroi, Y. Nakagawa, K. Someya, K. Iwatani, Y. Sawa, H. Takahashi, M. Honda, J. Kunisawa, H. Kiyono, HIV mucosal vaccine: nasal immunization with gp160-encapsulated hemagglutinating virus of Japan-liposome induces antigen-specific CTLs and neutralizing antibody responses, J. Immunol. 170 (1) (2003) 495–502.

[23] K. Yachi, H. Harashima, H. Kikuchi, R. Sudo, H. Yamauchi, K. Ebihara, H. Matsuo, K. Funato, H. Kiwada, Biopharmaceutical evaluation of the liposomes prepared by rehydration of freeze-dried empty liposomes (FDELs) with an aqueous solution of a drug, Biopharm. Drug Dispos. 17 (7) (1996) 589–605.

[24] S. Sakuma, N. Suzuki, R. Sudo, K. Hiwatari, A. Kishida, M. Akashi, Optimized chemical structure of nanoparticles as carriers for oral delivery of salmon calcitonin, Int. J. Pharm. 239 (1–2) (2002) 185–195.

[25] N. Pante, M. Kann, Nuclear pore complex is able to transport macromolecules with diameters of about 39 nm, Mol. Biol. Cell 13 (2) (2002) 425–434.

[26] Z. Shen, G. Reznikoff, G. Dranoff, K.L. Rock, Cloned dendritic cells can present exogenous antigens on both MHC class I and class II molecules, J. Immunol. 158 (6) (1997) 2723–2730.

[27] M. Nakanishi, H. Mizuguchia, K. Ashihara, T. Senda, T. Akuta, J. Okabe, E. Nagoshi, A. Masago, A. Eguchi, Y. Suzuki, H. Inokuchi, A. Watabe, S. Ueda, T. Hayakawa, T. Mayumi, Gene transfer vectors based on Sendai virus, J. Control. Release 54 (1) (1998) 61–68.

[28] D.P. Howell, R.J. Krieser, A. Eastman, M.A. Barry, Deoxyribonuclease II is a lysosomal barrier to transfection, Molec. Ther. 8 (6) (2003) 957–963.

[29] C.M. Wiethoff, C.R. Middaugh, Barriers to nonviral gene delivery, J. Pharm. Sci. 92 (2) (2003) 203–217.

[30] Y. Ogawa, Injectable microcapsules prepared with biodegradable poly(alpha-hydroxy) acids for prolonged release of drugs, J. Biomater. Sci., Polym. Ed. 8 (5) (1997) 391–409.

[31] S.B. La, T. Okano, K. Kataoka, Preparation and characterization of the micelle-forming polymeric drug indomethacin-incorporated poly(ethylene oxide)-poly(beta-benzyl L-aspartate) block copolymer micelles, J. Pharm. Sci. 85 (1) (1996) 85–90.

[32] J. Kunisawa, A. Okudaira, Y. Tsutusmi, I. Takahashi, T. Nakanishi, H. Kiyono, T. Mayumi, Characterization of mucoadhesive microspheres for the induction of mucosal and systemic immune responses, Vaccine 19 (4–5) (2000) 589–594.

[33] J. Panyam, W.Z. Zhou, S. Prabha, S.K. Sahoo, V. Labhasetwar, Rapid endo-lysosomal escape of poly(DL-lactide-co-glycolide) nanoparticles: implications for drug and gene delivery, FASEB J. 16 (10) (2002) 1217–1226.

[34] V.P. Torchilin, R. Rammohan, V. Weissig, T.S. Levchenko, TAT peptide on the surface of liposomes affords their efficient intracellular delivery even at low temperature and in the presence of metabolic inhibitors, Proc. Natl. Acad. Sci. U. S. A. 98 (15) (2001) 8786–8791.

[35] V.P. Torchilin, T.S. Levchenko, R. Rammohan, N. Volodina, B. Papahadjopoulos-Sternberg, G.G. D'Souza, Cell transfection in vitro and in vivo with nontoxic TAT peptide–liposome–DNA complexes, Proc. Natl. Acad. Sci. U. S. A. 100 (4) (2003) 1972–1977.